From Micro- to Nano-Multifunctional Theranostic Platform: Effective Ultrasound Imaging Is Not Just a Matter of Scale

From Micro- to Nano-Multifunctional Theranostic Platform: Effective Ultrasound Imaging Is Not Just a Matter of Scale

Sara Zullino, Monica Argenziano, Ilaria Stura, Caterina Guiot and Roberta Cavalli

Abstract

Ultrasound Contrast Agents (UCAs) consisting of gas-filled-coated Microbubbles (MBs) with diameters between 1 and 10 mm have been used for a number of decades in diagnostic imaging. In recent years, submicron contrast agents have proven to be a viable alternative to MBs for ultrasound (US)-based applications for their capability to extravasate and accumulate in the tumor tissue via the enhanced permeability and retention effect. After a short overview of the more recent approaches to ultrasound-mediated imaging and therapeutics at the nanoscale, phase-change contrast agents (PCCAs), which can be phase-transitioned into highly echogenic MBs by means of US, are here presented. The phenomenon of acoustic droplet vaporization (ADV) to produce bubbles is widely investigated for both imaging and therapeutic applications to develop promising theranostic platforms.

Keywords

nanobubbles, therapeutic ultrasound, ultrasound contrast agents, drug delivery, acoustic droplet vaporization

Introduction

The goal of nanoscale theranostics is to reach targeted tissues and cells for delivering any cargo of interest (drugs, proteins, and DNA) and visualizing in real time the actual achievement of the task. Nanoscale dimensions are required for internalization of the carrier by cells, or for trespassing of anatomical, and/or functional membranes such as the skin, or the blood–brain barrier. Nanocarriers of different materials and characteristics have been so far proposed. Their design can be driven taking into account either the cells to be targeted or the visualization approach, for example, ultrasound (US),[1] magnetic resonance imaging (MRI),[2] and photoacoustic imaging (PAI).[3-5]

Being sensitive to variations in density and compressibility with respect to the surrounding medium, traditional US imaging requires the presence of acoustical scatterers. A very large deal of literature has been devoted to gas-filled microbubbles (MBs). As a matter of fact, MBs have been extensively used in the past as ultrasound contrast agents (UCAs). While their shell has been manufactured using different materials (polymers, lipids, or proteins), their core was mainly composed by inert and nontoxic gases, such as perfluorocarbons (PFCs), which have a very low solubility in blood. Many MBs were approved by the Food and Drug Administration (FDA) in the United States and the European Medicines Agency (EMA) in Europe and are commercially available since 20 years. Consequently, the increasing interest of the clinicians for an extensive application in medicine pushed the US equipment producers to develop ad hoc imaging techniques, such as contrast-enhanced US, to optimize the US backscattered reflection.

Such experience suggested the idea of manufacturing nano-sized carriers able to permeate tissues and then to perform some phase change to become visible and monitorable by US medical sonography. Retracing the history of UCAs may be useful to arouse new ideas for future developments.

Ultrasound Contrast Agents

According to the core composition, UCAs can be divided into three main categories: (1) gas core, (2) liquid core, and (3) solid

Abbreviations

ADV	Acoustic Droplet Vaporization
APM	Activation Pressure Matching
BBB	Blood Brain Barrier
BSA	Bovine Serum Albumin
CEUS	Contrast Enhanced Ultrasound
CHL	Chlorambucil
DAPI	4′,6-diamidino-2-phenylindole
DFB	Decafluorobutane
DFP	2H,3H-perfluoropentane
DOX	Doxorubicin
DTX	Docetaxel
EMA	European Medicines Agency
EPR	Enhanced Permeability and Retention
ESW	Extracorporeal Shock Wave
ESWs	Extracorporeal Shock Waves
FDA	Food and Drug Administration
Gd	Gadolinium
Gd-DOTP	Gd(DOTP)5-(1,4,7,10-tetra-azacyclododecane-N,N′,N″,N‴-tetrakis(methylenephosphonic acid))
IC	Inertial Cavitation
LIFU	Low-Intensity Focused Ultrasound
MB	Microbubble
MBs	Microbubbles
MI	Mechanical Index
MRI	Magnetic Resonance Imaging
MWA	Microwave Ablation
NB	Nanobubble
NBs	Nanobubbles
ND	Nanodroplet
NDs	Nanodroplets
NIR	Near-Infrared
NP	Nanoparticle
NPs	Nanoparticles
OFP	Octafluoropropane
OLND	Oxygen Loaded Nanodroplet
OLNDs	Oxygen Loaded Nanodroplets
PA	Photoacoustics
PAI	Photoacoustic Imaging
PCCA	Phase Change Contrast Agent
PCCAs	Phase Change Contrast Agents
PCI	Phase Contrast Imaging
PEG-PCL	Poly(ethylene glycol)-co-polycaprolactone
PEG-PLLA	Poly(ethylene oxide)-co-poly(l-lactide)
PFC	Perfluorocarbon
PFCE	Perfluoro-15-crown-5-ether
PFCs	Perfluorocarbons
PFH	Perfluorohexane
PFP	Perfluoropentane
PLGA	Poly(lactide-co-glycolide)-co-poly(ethylene glycol)
PLP	Prednisolone Phosphate
PMCH	Perfluoromethylcyclohexane
PNP	Peak Negative Pressure
PTX	Paclitaxel
PVA	Poly(vinyl alcohol)
SF6	Sulfur Hexafluoride
SPION	Superparamagnetic Iron Oxide Nanoparticle
SPIONs	Superparamagnetic Iron Oxide Nanoparticles
UCA	Ultrasound Contrast Agent
UCAs	Ultrasound Contrast Agents
US	Ultrasound
UV	Ultraviolet

contrast agents. All of them present a density and compressibility substantially different from that of blood and tissues. MBs belong to the first class: they have a gas core surrounded by a shell and their size is usually on the order of a few microns. Upon US application, they not only enhance US backscattering but they can oscillate in the sound field, producing a nonlinear acoustic signal enabling the selective detection of the echoes from the MBs from those of surrounding tissue.[6] Recently, nanosized bubbles have been investigated.[22] Different types of liquid core contrast agents for US imaging have been prepared, tuning composition and size. Liposomes and PFC droplets are the most used nanoscale systems. Liposomes consist of a lipid bilayer with a hydrophilic liquid core. Air pockets within the lipid bilayer can generate acoustic reflectivity.[7] Nanodroplets (NDs) are US-triggered phase-change contrast agents (PCCAs) and their unique properties are discussed in the following sections of this review. Finally, solid nanoparticles (NPs) such as amorphous solid particles, including silica or iron oxide particles, can contain gas cavities in their pore structure. They showed the capability to generate detectable backscatter for US imaging.[8] Due to their size, nanoscale UCAs offer some advantages with respect to MBs, such as their ability to extravasate, providing the opportunity to image targets beyond the vascular system. Concerning liquid/solid UCAs, the relative incompressibility of their core produces a low acoustic reflectivity, making their detection somehow difficult. An overview on UCAs, their main properties, and structure is shown in Table 1 and Figure 1.

MBs: From Diagnosis to Therapy

MBs are blood pool contrast agents because they are transported after intravenous injection in the bloodstream being unable to extravasate due to their size (1-10 mm).[38]

According to the Rayleigh description, US backscattering depends on a combination of two factors: the high compressibility of the gas core and the different density with respect to the background. Whenever a sound wave hits such gaseous particles in a liquid medium, the difference between their acoustic impedance becomes remarkable, thus resulting in a stronger echo and greater acoustic energy detectable by standard sonoghaphy. Following insonation, MBs behave as very efficient US scatterers: they start to compress and expand as the gas responds to the pressure oscillations of the acoustic wave.[1,39] When properly modulated, US may elicit nonlinear acoustic signals for selective echoes detection.[6] Since bubble deletion occurs in the bloodstream and may prevent distal detection, the MB stability is crucial, and since 1990, several types of UCAs have been developed to improve bubble lifetime. Albunex (Molecular Biosystems, San Diego, California) was the first UCA available on the market in 1994. It consisted of air bubbles encapsulated by a human albumin shell with the aim of increasing stability.[40] Since then, many other agents have been introduced in clinical practice. Currently, the majority of the UCAs has a lipid coating and contains gases with low diffusivity in blood to further increase bubble half-life. The gases used in commercially available UCAs are sulfur

Table 1. Overview on Contrast Agents Used in US Imaging and Their Main Properties.

	Microbubble	Liposome	Nanobubble	Nanodroplet	Nanoparticle
Core	Gas (air, PFC, SF_6)	Hydrophilic liquid	Gas (air, PFC, SF_6)	Liquid (PFC)	Gas (PFC)
Shell	Phospholipid, polymer, protein	Lipid bilayer	Polymer, lipid	Polymer, lipid	Mesoporous silica
Size	1-10 mm	100 nm-10 mm	200-800 nm	200 nm-1 mm	50-500 nm
References	9-12	13-17	18-22	23-30	31-37

Abbreviations: US, ultrasound; PFC, perfluorocarbon; SF_6, sulfur hexafluoride.

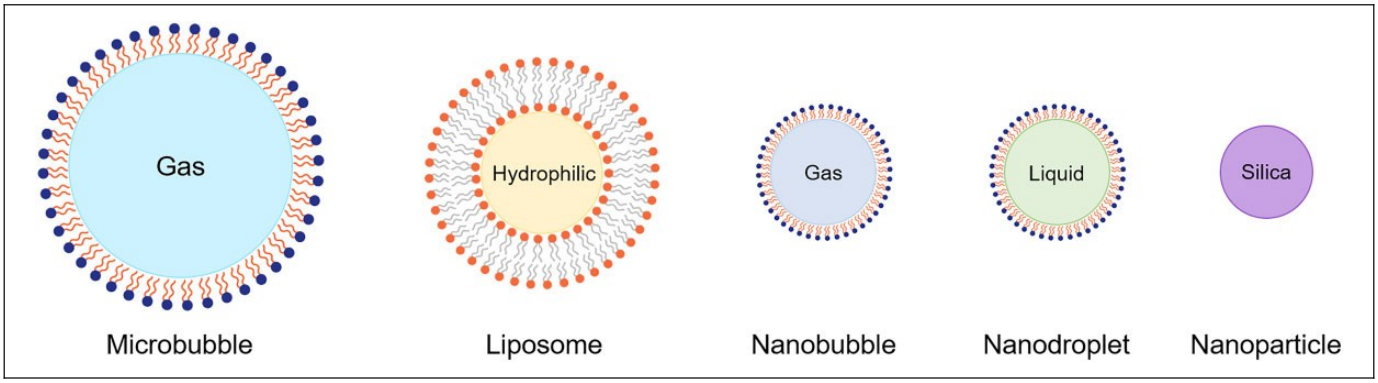

Figure 1. Schematic core–shell structure of contrast agents used in molecular US imaging (not to scale). US indicates ultrasound.

hexafluoride in Sonovue/Lumason (Bracco Imaging, Milan, Italy),[41] octafluoropropane (OFP) (C_3F_8) in Definity/Luminity® (Lantheus Medical Imaging, North Billerica, Massachusetts),[42] and decafluorobutane (DFB; C_4F_{10}) in Sonazoid (Daichii Sankyo, GE Healthcare, Tokyo, Japan).[43] Following Albunex, a new albumin-based formulation was developed encapsulating OFP, named Optison (GE Healthcare AS, Oslo, Norway).[44] However, albumin results in a rather thick and rigid coating,[12] which limits bubble oscillations. On the contrary, lipid-coated bubbles, being the shell more flexible, allow relatively large oscillations,[9] whereas a polymer coating can increase the stability.[10] Nevertheless, polymer-coated contrast agents have more rigid shells, which need to be cracked in order to vaporize the oil core or let the gas escape, providing imaging contrast.[10,11] Both lipids and polymers offer more options to tune the chemical and mechanical properties of the shell, also giving more opportunities for functionalization and targeting of the bubbles.

Since 1990s, UCAs have attracted much research as carriers for drug delivery in order to transport drugs to specific diseased site and safely achieve the desired therapeutic effect, avoiding side effects. The benefit of using US in combination with MBs might be the delivering of the payload in a controlled way, by activating the release process only when the ultrasonic beam is switched on. Moreover, US can provide local real-time imaging.[45] These features allow a more specific delivery of the therapeutic agents, thus reducing the undesired side effects and improving the efficacy.

Generally, two modalities for drug delivery by UCAs are possible. In the co-administration approach, the UCAs are injected in the bloodstream alongside the therapeutic agent. Conversely, local US application can induce a transient

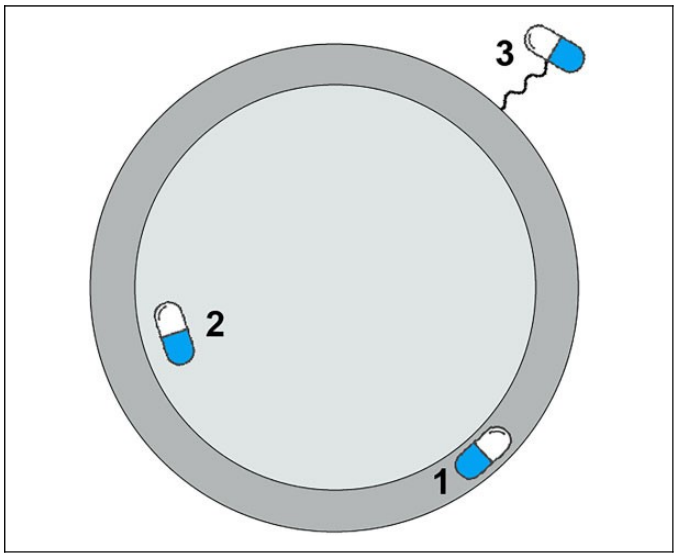

Figure 2. Simplified sketch of main drug-loading techniques in microbubbles/nanobubbles (not to scale). Drugs can be embedded in the shell (1), incorporated in the core, in the case of gases or molecules soluble in PFCs (2), covalently attached to the surface (3). PFCs indicates perfluorocarbons.

increase in endothelial cell membrane permeability, enhancing therapeutic agent uptake by the target cells.[46,47] This method is also known as sonoporation. So far, several MB loading strategies have been investigated and proposed, such as loading drugs into MB core, or incorporating drugs within the shell through covalent or noncovalent interactions (Figure 2).[48] Therefore, MBs can act as a reservoir, and the chemical properties of the drug can affect the release kinetics.[49]

Different MB formulations have been designed to promote the transport of hydrophilic as well as lipophilic therapeutic agents. The use of US as external trigger to improve drug delivery efficiency has been extensively studied, as reported by Kooiman et al.[50]

Hybrid core–shell MBs based on biodegradable cross-linked polymers and phospholipids were described by Capece et al.[51] A self-assembly process starting from the preparation of liquid vesicles was tuned to obtain this system. It involved three steps: (1) the deposition of a phospholipid monolayer around a PFC droplet; (2) the addition of a hydrophilic polymer grafted with a vinyl moiety; and (3) the free radical photopolymerization to cross-link the grafted vinyl side chains. These liquid vesicles, in the presence of US, could successfully undergo the liquid to gas transition, thereby transforming the polymer vesicles into MBs.

A variety of drug-loaded droplets able to undergo a US-driven phase change to gas MBs has been extensively investigated in literature. In vitro results showed the delivery of the lipophilic drug chlorambucil (CHL) encapsulated by albumin/soybean oil-coated microdroplets to hamster ovary cells.[52] The authors found that incubation with the CHL-loaded NDs emulsion exposed to US almost doubled growth inhibition.

For the sake of completeness, we also report the use of MBs as contrast agent in other imaging applications. Interestingly, coupling graphene with MB surface offered the possibility to enhance photoacoustic signals. Paradossi et al designed an hybrid system, made of pristine graphene tethered to poly(vinyl alcohol)-based MBs and demonstrated a very good enhancement in the near-infrared (NIR) spectral region of the photoacoustic signal.[4] The MBs-containing Gadolinium (Gd) complexes can be exploited to obtain a dual imaging strategy, for example, phase contrast imaging and MRI.[53] Superparamagnetic iron oxide NP-modified MBs for US-MRI bimodality imaging have been proposed as well.[54]

The Need for Smaller US-Monitorable Carriers

MBs are not able to passively extravasate due to their micron-scaled sizes, but they remain in the circulation until they are taken up by the spleen and the liver[55] or they dissolve in rather short times.[56] To overcome this limitation, nanosized formulations have been designed for US-triggered drug release outside the bloodstream.[49] In addition, MBs are too large to pass through the leaky vasculature of the tumor. Typically, tumor vessels are permeable from particles far lower than 1 mm, suggesting that the cutoff size of the pores is between 400 and 600 nm in diameter.[57] Based on these premises, targeting the tumor cell requires nanocarriers able to escape from the capillaries and enter the defective tumor microcirculation via the so-called enhanced permeability and retention (EPR) effect.[58] This feature can "per se" achieve drug accumulation in tumors without specific targeting ligands.

Nanoscale carriers may be designed as nanobubbles (NBs) or NDs, depending on whether the core is gaseous or liquid at room temperature. However, NDs show negligible nonlinear acoustic contrast due to the relatively incompressible liquid core.[59-61] Upon US, they can be phase transitioned into MBs, thus generating acoustic contrast locally.[23,24,62] Unless a recently proposed procedure of "condensation" from micron-sized UCAs,[63] NDs are normally manufactured via sonication,[28] high-shear homogenization,[64] or high-speed mechanical agitation.[52,65] Briefly, an aqueous solution or dispersion of coating material is emulsified by one of the techniques mentioned above in the presence of liquid PFCs. The NDs typically result in a polydisperse size distribution. Lately, microfluidics-based devices have been investigated, which allow a finer control of the droplet diameter and production rate, by controlling gas pressure, liquid flow rate, and device geometry.[66] Sheeran et al described a low-temperature extrusion method to emulsify liquid droplets filled by DFB. Since DFB at room temperature is a gas, droplet generation requires that condensation occurs at reduced temperatures and/or increased pressures. In this study, droplets were first produced by condensing DFB gas at very low temperatures and then by encapsulating the resulting liquid DFB in lipid shells by membrane extrusion. A postsonication step can be carried out to produce NDs with a more uniform size distribution.[24]

Sheeran et al investigated how to manufacture PCCAs containing highly volatile PFCs.[26] In their work, they showed that DFB (boiling point -2°C) can be incorporated into metastable liquid submicron droplets with proper encapsulation methods. The resulting droplets are activatable with substantially less energy than other more popular PFCs. Because DFB is a gas at room temperature, producing liquid DFB droplets by using conventional techniques, such as microfluidics-based devices, sonication, or homogenization, may be a challenge. The group of Sheeran proposed an alternative method of generating nanometer-sized lipid-coated droplets based on condensation of preformed MBs-containing DFB, through a combination of decreased environmental temperature and increased environmental pressure.[24] In the liquid state, the reduction in size to nanometer scale increases the Laplace pressure that, in turn, stabilizes the droplets against re-expansion at physiological temperature, unless an external trigger, such as US or heat, is applied. This method is known as "microbubble condensation" (Figure 3). In a subsequent investigation of MB condensation, Sheeran et al revealed the inherent tradeoffs involved with forming PCCAs from low-boiling point PFCs.[67] Martin et al proposed to accumulate perfluorocarbon NDs in a close-packed configuration and let them grow in size in situ, so that the phase-change conversion can occur at lower US pressures compared with isolated NDs.[68] Cavalli et al developed perfluoropentane (PFP)-cored polymer–lipid-coated NBs. They are a hybrid system containing a phospholipid monolayer at the NB interface, coated by a polymer shell to improve stability.[25] This type of formulation is referred to as "nanobubbles" for sake of simplicity, but it must be said that, prior to the US application, it would be more accurate to use the term "nanodroplets" when the core is constituted of PFP, being the PFC liquid at room temperature (boiling point 29°C).[69] The rationale of the

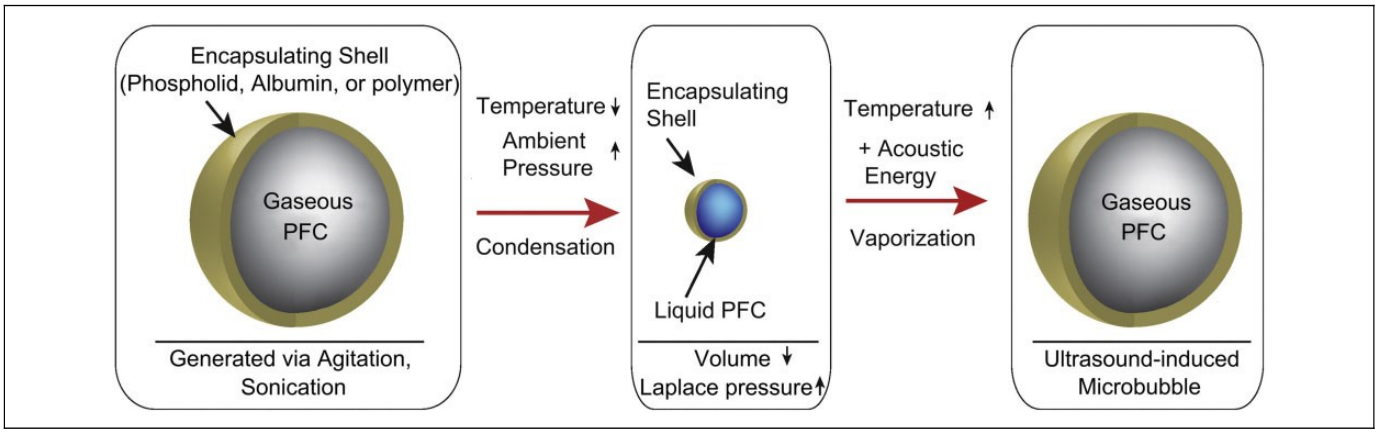

Figure 3. The exposure of preformed PFC MBs to decreased ambient temperature and increased ambient pressure results in condensation of the gaseous core. The decreased size results in an increased Laplace pressure, which serves to preserve the particle in the liquid state. Once exposed to increased temperature and energy delivered via US, vaporization of the droplet core results in a larger, highly echogenic gas MBs. PFC indicates perfluorocarbon; MBs, microbubbles. Reprinted from *Biomaterials*, Vol. 33, Sheeran PS, Luois SH, Mullin LB, Matsunaga TO, Dayton PA. Design of ultrasonically-activatable nanoparticles using low boiling point perfluorocarbons, 3262-3269, Copyright (2012), with permission from Elsevier.

hybrid lipid/polymer system is that phospholipid monolayers can adsorb charged polymers, such as polysaccharides exploiting various type of interactions.[70] Moreover, the addition of cosurfactant molecules to the phospholipid monolayer can play a synergic effect on the interfacial packing and surface tension. Shells of various thicknesses can be developed, and multilayer systems can be obtained by the layer-by-layer deposition method.

NDs need to be stabilized to prevent coalescence. Most PCCAs are stabilized by either a single type of phospholipid,[26] a mixture of them,[27] or are entirely formulated of block copolymer.[28] In 2000, Kripfgans et al reported preliminary results for manufacturing albumin-coated droplets and studied their evaporation as a function of the applied acoustic pressure and frequency, together with a simulation predicting their lifetime based on gas diffusion.[65] Three years later, the idea of producing albumin-coated and other PFC-cored microdroplets undergoing US-mediated cavitation was investigated by Giesecke and Hynynen by in vitro determination of the inertial cavitation (IC) thresholds at various frequencies.[70] A recent study by Lee et al suggested that coating the NDs with a protein–polymer shell can improve their stability.[29] Capece et al studied the interface of hybrid shelled droplets encapsulating 2H,3H-decaperfluoropentane (DFP).[30] Droplet fabrication was based on the deposition of a dextran methacrylate layer onto the surface of surfactants. The droplets have been stabilized against coalescence by ultraviolet curing, introducing cross-links in the polymer layer, and transforming the shell into an elastomeric membrane with viscoelastic behavior. Following US exposure, the DFP core of the droplets vaporized transforming the particles into MBs. The presence of a robust cross-linked polymer shell conferred an unusual stability also during the core phase transition and allowed the recovery of the initial droplet state within a few minutes after switching off US.

PFCs have proven to be good candidates for liquid emulsions because they have low solubility in aqueous media and are nontoxic in small doses.[72,73] Due to their immiscibility in water, high-molecular weight, and low-surface tension, PFC-cored droplets can remain stable in circulation much longer than their gas-cored counterparts of similar size.[74] Depending on the PFC of choice, the resulting half-life in vivo ranges from hours to days,[75] which is an appealing feature for applications involving passive targeting and/or drug delivery. Low-boiling point PFCs, such as PFP, are particularly attractive because they allow the NDs to be designed in a metastable, "superheated" state from which they can rapidly turn to gas bubbles in response to US. Table 2 lists selected PFCs that have been used for ultrasonically activatable contrast agents along with their physical properties, whether available, collected from several resources of literature.[76,77] Therefore, these NDs are often called PCCAs[78] and the phenomenon is known as acoustic droplet vaporization (ADV).

Finally, many solid nanocarriers have been introduced so far. The use of porous silica NPs to enhance the ND stability has been proposed as well.[94]

Applications in Nanomedicine

Molecular Imaging of Cancer

One of the most important goal in tumor diagnosis is the early detection of cancer, for both primary tumors and metastasis. Two techniques can be used to achieve this goal. First, being tumor vasculature defective and characterized by wide fenestrations, leaking of nanocarriers makes the tumor detectable by imaging.[95] Second, the imaging agent can be functionalized with specific antibodies able to identify and bind the cells overexpressing the cancerous phenotype. Theoretically, targeted NDs can penetrate the endothelial barrier and bind those tumor cells.[96]

Table 2. Physico-chemical Properties of Selected PFCs Used for Liquid Nanoemulsion.

Name	Abbreviations	Chemical Formula	bp (°C)	Molecular Weight (g/mol)	Liquid Density (kg/m^3)	Surface Tension (mN/m)	References
Octafluoropropane[a]	OFP	C_3F_8	–36.7	188.02	—	—	67,79
Decafluorobutane[a]	DFB	C_4F_{10}	–1.7	238.03	—	—	24,26,67,79-83
Perfluropentane	PFP	C_5F_{12}	29	288.03	1630	9.50	23,26,28,52,65,84-90
Perfluorohexane	PFH	C_6F_{14}	56.6	338.04	1669	12.23	26,86,90,91
Perfluoroheptane	FC84	C_7F_{16}	80	388.05	1680	13.55	—
Perfluorooctane	PFO	C_8F_{18}	101	438.06	1730	14.47	91
Decafluoropentane	DFP	$C_5H_2F_{10}$	55	252.05	1600	14.10	92
Perfluoro(2-methyl-3-pentaone)	PFMP	$C_6F_{12}O$	49	316.04	—	—	26
Perfluoro-15-crown-5-ether	PFCE	$C_{10}F_{20}O_5$	146	580.07	—	—	93

Abbreviations: PFC, perfluorocarbon; bp, boiling point.
[a]PFC in gaseous state at 25°C.

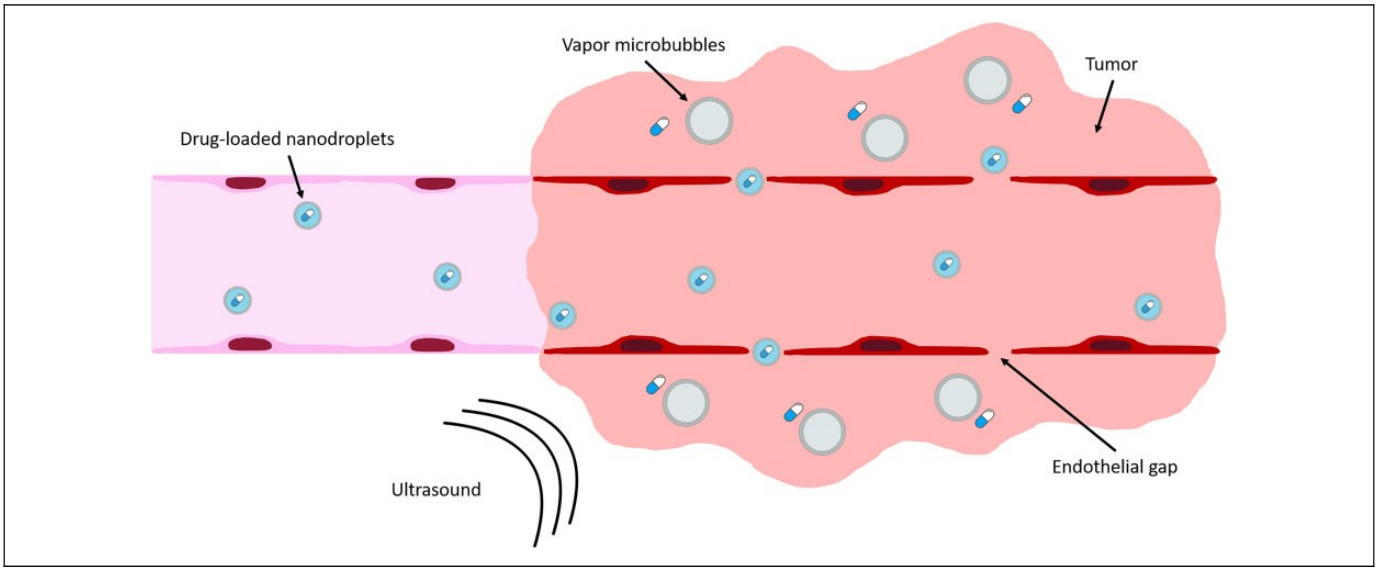

Figure 4. Schematic representation of chemotherapeutic delivery through the defective tumor microvasculature using drug-loaded ND (not to scale). Hydrophobic drugs can be stored in the NDs cores. The tight junctions between endothelial cells in normal tissues do not allow extravasation of drug-loaded NDs. In contrast, tumors are characterized by fenestrated vasculature with large gaps between the endothelial cells, which allows drug-loaded nanodroplets to pass and accumulate in the tumor interstitium. US causes the NDs to evaporate into MBs, thus locally generating acoustic contrast and triggering the release of the drug. NDs indicates nanodroplets; US, ultrasound; MBs, microbubbles.

Animal model experiments have demonstrated that ADV-based angiography can be used as real-time monitoring of the effect of the ultrasonic therapy in pancreatic cancer, breast cancer models, and kidney function.[93,97] Matsuura and colleagues used quantum dots incorporated in PFC droplets to show that they can act as additional cavitation nuclei within the core and appear to significantly decrease ADV threshold.[98] They suggested the idea that NP-loaded imaging agent may help in spatially and temporally controlling NP deposition: this approach paved the way to extend ADV-based imaging to other applications.

Therapeutic Delivery

The therapeutic strategy based on the interaction between drug-loaded NDs and US was first proposed in anticancer chemotherapy, for which temporal and spatial control of drug distribution is a goal. With respect to MBs, submicron PCCAs represent a novel approach to achieve localized drug delivery due to their unique properties. The EPR effect in solid tumors assumes that extravasation occurs from the capillaries through their nanometric porous structure (Figure 4).

Tumor therapy with drug-loaded PFC nanoemulsions combined with US was studied in vitro and in vivo. Gao et al manufactured and characterized multifunctional NPs that combine the properties of polymeric drug carriers, US imaging contrast agents, and enhancers of US-mediated drug delivery.[99] At room temperature, the systems comprise PFC NDs stabilized by biodegradable block copolymer poly(ethylene oxide)-co-poly(l-lactide) or poly(ethylene glycol)-co-polycaprolactone shell. Upon heating to physiological temperatures, the NDs convert into NBs/MBs. Following intravenous injections, a longlasting,

strong, and selective US contrast was observed in the tumor volume, indicating NB extravasation through the defective tumor microvasculature, suggesting their coalescence into larger, echogenic MBs in the tumor tissue. Under the action of tumor-directed US, MBs cavitate and collapse releasing the encapsulated doxorubicin (DOX) and dramatically enhanced intracellular drug uptake by breast cancer cells in vivo. Rapoport et al also developed polymeric micelles to encapsulate liquid PFP containing DOX. Increasing the temperature to 37°C caused the PFP nanodrops to vaporize into larger bubbles. It was proposed that US focused on the tumor could generate larger MBs formed by coalescence of the vaporized NDs. The authors showed the feasibility of using polymer-stabilized perfluoropentane NDs to deliver DOX to breast cancer xenograft tumors, proving that tumor growth could be arrested by this method.[19] In vitro US-triggered delivery of paclitaxel (PTX) to monolayers of prostate cancer cells was successfully reported for lipid-coated perfluorohexane (PFH) NDs.[86]

In a very recent paper, Cao et al introduced phase-changeable drug delivery NDs with programmable low-intensity focused ultrasound (LIFU) that could trigger drug release significantly, enhancing anticancer drug delivery. Based on the difference of acoustic pressure between soft-shelled and hard-shelled nanosystems, lipid-based and poly(lactide-co-glycolide)-co-poly(-ethylene glycol) (PLGA)-based NDs with encapsulated PFP and anticancer drug DOX were manufactured. By accurate acoustic energy deposition and coadministration of multiple NDs, a programmable drug-releasing profile was achieved, which could efficiently increase therapeutic effectiveness and decrease the course of chemotherapeutic treatment, as the authors demonstrated by both in vitro and in vivo studies.[100] The DOX-loaded acoustic phase-change NDs were developed for combined physical antivascular therapy and chemotherapy. The US stimulation can simultaneously induce locally vascular permeability and trigger drug release.[101] Recently, Marano et al published that glycolchitosan NDs loaded with PTX or docetaxel can target taxanes to castration-resistant prostate cancer cell lines.[102] Upon extracorporeal shock waves, NDs entered two different castration-resistant prostate cancer cells (PC3 and DU145), leading to higher cytotoxic and antimigration effect.

Although most of the research was devoted to cancer, other applications were also investigated. Prato et al introduced a new platform of oxygen nanocarriers, with DFP core and dextran shell which showed good oxygen carrying capacity, and no toxic effects on human keratinocytes after cell internalization, suggesting that US-activated nanocarriers might be used to topically treat hypoxia-associated pathologies of the cutaneous tissues.[92,103] Oxygen-loaded nanodroplets (OLNDs) are also internalized by cancer cells (eg, TUBO cells) and are localized only in the cytoplasm compartment (Figure 5). This result indicates that OLNDs are able to deliver their payload directly inside the cancer cells, minimizing the damage to the surrounding healthy tissue.

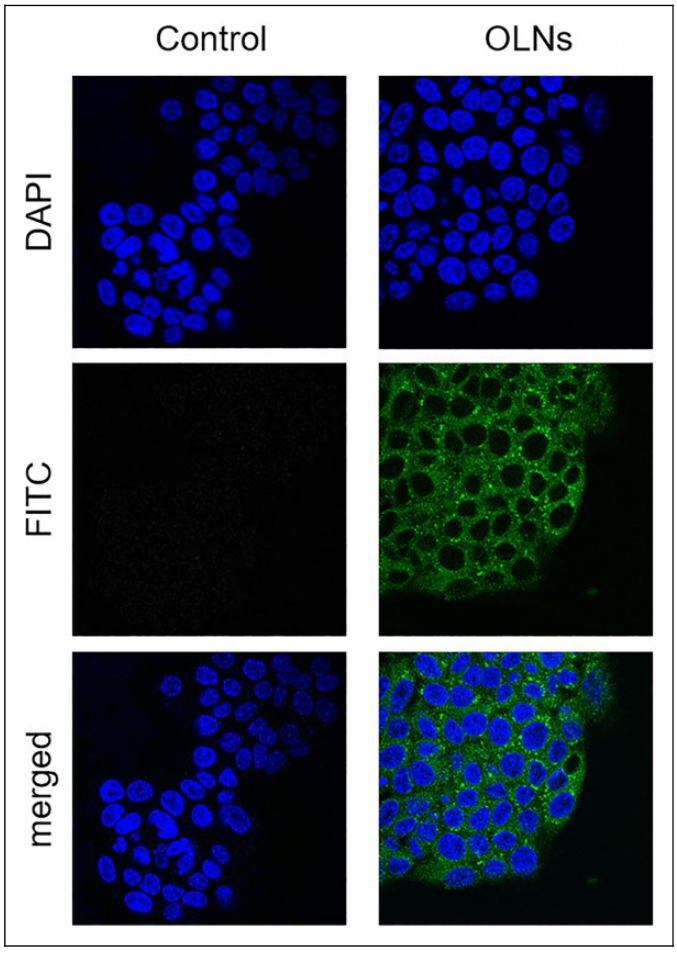

Figure 5. OLNDs internalization by TUBO cell line. TUBO cells were left untreated (left panels) or treated with FITC-labeled OLND PBS formulation (right panels) for 24 hours in normoxia. After DAPI staining, cells were imaged by confocal microscopy. Results are shown as representative images from three independent experiments. Top panels: Cell nuclei after DAPI staining (blue). Central panels: FITC-labeled OLND (green). Bottom panels: Merged images. Magnification × 63. OLNDs indicates oxygen-loaded nanodroplets; FITC, fluorescein isothiocyanate; PBS, phosphate-buffered saline; 4′,6-diamidino-2-phenylindole (DAPI).

Ultrasound as external trigger to enhance the gene transfection efficiency has been investigated as well because of its safety and noninvasiveness for site-specific targeting, overmatching the other physical methods.[104] Gao et al developed an US-triggered phase-transition cationic ND based on a novel perfluorinated amphiphilic poly(amino acid), which could simultaneously load PFP and nucleic acids.[105] Cavalli et al developed a polymeric ND formulation, consisting of a chitosan-based shell and a PFP core for DNA delivery.[64] To obtain a nanoscale system, tetradecylphosphoric acid (C14) was added to the formulation. This amphiphilic molecule can localize to the PFP–water interface, lowering the surface tension. Chitosan was selected for the ND shell because of its low toxicity, low immunogenicity, and excellent biocompatibility. DNA-loaded NDs showed the ability to complex with and protect DNA. Transfection of COS7 cells in vitro was triggered by US, without affecting cell viability.

Theranostics

Theranostic systems provide imaging support to a therapeutic treatment, offering the potential to image the pathological tissues and simultaneously to monitor the delivery kinetics and biodistribution of a drug. The MBs/NBs have been proposed as multifunctional theranostic agents with the capability to provide US imaging and US-triggered therapy. Oddo et al designed a multimodal theranostic platform based on poly(vinyl alcohol)-shelled MBs coupled with superparamagnetic iron oxide NPs and an NIR fluorescent probe (indocyanine green) in order to support MRI and fluorescence imaging capability.[106] Various PLGA-shelled NB formulations have been investigated as theranostic system for imaging and tumor drug delivery.[107-111] Rapoport et al have proposed a multifunctional imaging and treatment platform using nanosized PCCAs bearing a drug in the polymer shell in conjuction with drug-loaded micelles. Ultrasound, causing the PCCAs to vaporize, enhances local drug delivery, and the newly formed MBs can be used to monitor "on-the-fly" the effectiveness of the therapeutic treatment.[19] Cavalli et al developed a chitosan-based NB formulation, containing prednisolone phosphate as model drug and the paramagnetic complex 1, 4, 7, 10-tetra-azacyclododecane-N,N′,N″,N‴-tetrakis (methylene-phosphonic acid) (Gd-DOTP) as T1-MRI agent.[25] In a recent work, porphyrins were combined with pluronic NBs to obtain an US-activated theranostic agent that exploits the sonodynamic activity in vitro.[112] Recently, cell-penetrating peptide targeted 10-hydroxy camptothecin-loaded lipid NPs were combined with LIFU for precision theranostics against hepatocellular carcinoma. A hyaluronic acid-mediated tumor accumulation was observed and after irradiation by LIFU, NPs turned into MBs by ADV, thereby enhancing US imaging and promoting local release of antitumor drug.[113]

The Physics of ADV

The physical principles underlying ADV have not been completely clarified yet. Concerning the basic thermodynamics, in any closed system at a given temperature, the vapor pressure is defined as the pressure at which the liquid phase of a substance is in equilibrium with its vapor phase.

When the surrounding pressure is larger than the vapor pressure, the liquid substance remains in its condensed form. Conversely, when the surrounding local pressure drops below the vapor pressure, the liquid molecules will quickly escape from the gas phase (boiling) without any necessary changes in temperature.[114] The acoustic waves can modify the local pressure of the liquid, thus triggering the phase transformation, either from liquid to gas or backward from gas to liquid.

The Role of the Laplace Pressure

Being the ND a confined system, it experiences a Laplace pressure, which is defined as the pressure upon the interior fluid generated by the surface tension (or interfacial energy) between the two immiscible phases that compresses the liquid or gas inside the droplet:

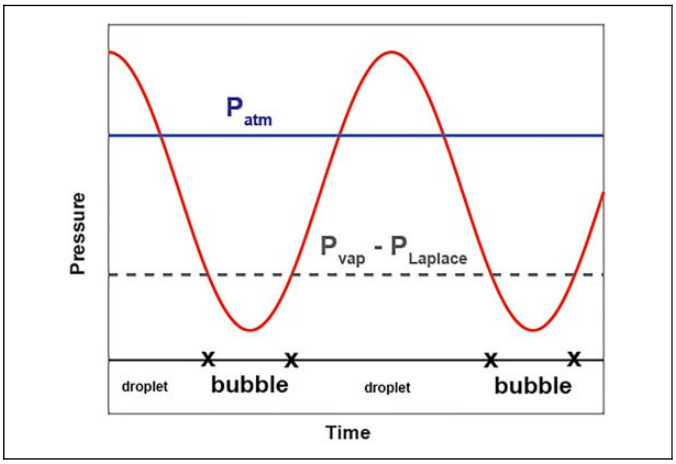

Figure 6. Schematic plot showing the vaporization of the liquid droplet as soon as the local acoustic pressure drops below the pressure difference between the vapor pressure and the Laplace pressure (not to scale).

$$\Delta P = P_{inside} - P_{outside} = \frac{2\sigma}{r(t)} \quad (1)$$

where P_{inside} and $P_{outside}$ indicate the pressure inside and outside a droplet, respectively, g is the interfacial tension, and $r(t)$ is the droplet radius. The hydrophobicity of liquid PFCs leads to relatively high interfacial surface tension when dispersed in water. During the phase of rarefactional acoustic pressure, the pressure within the PFC droplet drops below the vapor pressure of the PFC (called "subpressurization"): this event allows the liquid to transiently vaporize and condense back again at larger acoustic pressure (Figure 6). However, because the Laplace pressure is an inverse function of the radius, expansion of droplets in the nanometer range occurs less easily than in the micrometer range. NDs may experience Laplace pressures of the order of some atmospheres and actually PFC droplets injected in vivo do not vaporize spontaneously and hence their boiling point increases.[41] Lower boiling point PFCs, such as PFP, enable vaporization using lower acoustic amplitude.[42] Furthermore, liquid droplets immiscible in the surrounding liquid medium, because of the Laplace pressure, can experience "apparent superheating" and thus will never turn to a gas bubble if encapsulated by a nanoscale shell.

Finally, other authors reported subpressurization of liquid PFC droplets with no gas formation.[19,28,65,82] This phenomenon could be referred to "apparent subpressurization" (analogous to the apparent superheating) in which the Laplace pressure was sufficiently large that the vapor pressure at a temperature above the normal boiling point was still not greater than the local pressure inside the droplet. This may be due to the absence of a nucleation event.[114,115]

The Impact of the US Parameters

Much discussion in the literature has been devoted to the mechanisms forcing a droplet to undergo a phase transition when US is applied and, in particular, to define its threshold.

ADV will be favored by increasing US frequency, pulse length, and peak-negative pressure (PNP) of the acoustic wave and by decreasing the Laplace pressure (both due to lower surface tension or larger droplet radius). Several authors experimentally confirmed these findings.[71,79,116] All these factors should be taken into account to optimize ADV process.

The relation between ADV and IC threshold, that is, when the sudden expansion and then rapid collapse of a gas bubble in response to a PNP occurs, was investigated by different groups.[71,91,117-119] Their experiments focused on albumin- or lipid-coated microdroplets and demonstrated that the ADV threshold was lower than the IC threshold, meaning that the droplet-to-bubble transition occurs in less extreme conditions than those required for IC. The IC threshold was monitored through passive acoustic detection of albumin-coated microdroplets loaded with different PFCS, including those with boiling point higher than that of PFP (ie, PFH and perfluoromethylcyclohexane).[71] The PFC droplets of higher molecular weights and boiling points did not show larger IC threshold and thus superheating is not required to cavitate the droplets with US bursts.[71] This result was later confirmed by Rapoport et al in experiments with perfluoro-15-crown-5-ether NDs: the US pressures required to trigger their vaporization were only slightly higher than those for PFP NDs.[93] Kawabata et al proposed to use the sequential phase shifting of multiple liquids with different boiling points.[119] They considered NDS containing a mixture of PFP and DFP that could be vaporized at diagnostic US frequency: by changing the ratio of DFP to PFP, the US intensity required to induce sonographically significant vaporization changed. The authors hypothesized that vaporization of DFP with higher boiling point was favored by the fact that PFP was already vaporized.[119] In 2009, Rapoport et al showed that indeed US-induced droplet-to-bubble transition was substantially catalyzed by large preexisting bubbles irradiated by low-frequency US.[28,120] These results suggested a new strategy for improving the efficiency of droplet-to-bubble transition not only by mixing PFCs of different boiling point but also by using polydisperse droplet size distributions.

Other Open Problems

The main reason why the physical mechanisms of ADV still remain elusive relies in the large mismatch between the US wavelength and the droplet size. Nevertheless, such discrepancy may be overcome by a new recently proposed mechanism.[121] This study reveals that ADV is initiated by a combination of two phenomena: highly nonlinear distortion of the acoustic wave before it hits the droplet and focusing of the distorted wave by the droplet itself. At high excitation pressures, nonlinear distortion causes the formation of superharmonics, whose wavelengths are of the order of magnitude of the droplet size. These superharmonics strongly contribute to the focusing effect; therefore, the proposed mechanism also explains the observed pressure thresholding effect. This interpretation was validated with experimental measurements of the positions of the nucleation spots captured with an ultrahigh-speed camera, and an excellent agreement with the theoretical prediction was observed.

Another critical issue depends on the initial vapor nucleation required for ADV to occur. The basic explanation for the formation of a gaseous nucleus in an infinite liquid is provided by the homogeneous nucleation theory. It is usually assumed that the initial cavity formation takes place instantaneously.[122] Due to this very fast transition and the extremely small size of the initial vapor seed (on the order of 10 nm),[89] the nucleation pocket may entirely vaporize the droplet before the event becomes observable with the detection systems currently available. Experimental results actually show that some time is required: the probability of homogeneous nucleation of a growing gas bubble is proportional to the time window (at constant subpressurization) and increases exponentially with the magnitude of subpressurization. In 2016, Mountford and Borden pointed out that the mechanism of homogeneous nucleation may be an alternative explanation for the metastability of superheated NDs. Interestingly, they compared the homogeneous nucleation theory with some ADV results,[123,124] showing that a possible explanation was due to the subharmonic focusing of the incident US waves at the droplet–water interface,[121,125] which would increase the local PNP experienced within the droplet and facilitate the phase transition.

Theoretical Modeling

Theoretical modeling of ADV has been carried out as well. One of the first analytical approaches has been proposed by Qamar et al,[126,127] who modeled bubble evolution from microdroplets contained in a rigid tube. Their results were compared with the experimental data of Wong et al for PFP droplets.[125] The simulations by Qamar et al showed an interesting pattern by which under certain conditions, droplet evolution may be characterized by an overexpansion and oscillatory settling to a final diameter. Moreover, they assumed that the PFC mass evaporation rate was constant over the entire process of vaporization, which is a strong simplification, especially when the ambient pressure changed in response to the applied US field. Additionally, Qamar et al used the ideal gas law for describing the vapor bubble. More recently, Shpak et al proposed a simple model to describe the growth of a vapor bubble inside a PFP droplet,[128] hypothesizing that the vapor temperature inside the bubble is constant and equal to the boiling point for PFP (29°C at atmospheric pressure), and the bubble growth is driven by heat transfer from the surrounding liquid medium which has a temperature higher than that within the bubble. To compute the heat transfer, Shpak et al assumed a temperature gradient only within a thin (relative to the bubble radius) thermal boundary layer, whose thickness increases proportionally to the square root of time.[129,130] To take into account for the impact of US, they also included an effect called "rectified heat transfer."[131] In another study, Shpak et al[132] modeled the growth of a vapor bubble by numerically solving the Keller-Miksis equation[133] in combination with the standard partial differential equations, describing the temperature field in the surrounding liquid, the

heat transfer between the bubble and the liquid, and the gas diffusion through the bubble surface.[134] Regarding thermal processes, their model reproduces the approach used by Hao and Prosperetti for vapor bubbles in ordinary liquids.[135] Both models of Shpak et al assume that a vapor bubble is embedded in an infinite medium of liquid PFP, preventing the study of the bubble oscillations. The droplet-to-bubble transition has been modeled by Pitt et al who proposed a modification of the Rayleigh-Plesset equation.[136] Conversely to the models mentioned above, they considered a vapor bubble formed around a PFC droplet immersed in water, that is, the gas bubble formation initiates as a spherical vapor layer between the droplet surface and water and consists of a mixture of PFC and water vapor.

US Imaging Applications of ADV: Limitations and Perspectives

Many strategies using nanoscale systems have been proposed in order to improve the current formulations. As a matter of fact, some critical issues related to ADV at the nanoscale should be taken into account for future diagnostic and therapeutic applications. According to Laplace law, the smaller the droplet, the larger the internal pressure, thus increasing the saturation pressure required to trigger the droplet-to-bubble transition to higher temperature and acoustic pressure that are potentially harmful in clinical applications. The problem has been handled using different strategies ranging from droplet design to optimization of the US activation parameters.

In order to prevent the increase in ADV thresholds that occurs when the droplet size decreased, the use of volatile PFC has been proposed. The advantage in the vaporization thresholds obtained by increasing PFC volatility is, however, counterbalanced by a decrease in thermal stability (as the vaporization pressure and temperature are governed by the Clausius-Clapeyron relation). The stability of NDs can be improved with surfactant or stabilizing agent in the external media,[19,28,96,96,137] but the in vivo stability is still critical, due to the rapid dilution of the surfactants upon injection. In an early study by Kawabata et al, the authors showed that the ADV threshold can be finely tuned by mixing miscible PFC.[119] Some years later, Sheeran et al manufactured droplets composed of 1:1 mixture of DFB and OFP and showed that the resulted droplets had intermediate vaporization thresholds as well as intermediate stability.[67] Another strategy to lower the phase-transition threshold is to increase the size of the NDs.[71,116,118] Larger droplets are characterized by smaller Laplace pressure[138] and are more easily vaporized into bubbles at lower pressure with respect to nanoscale droplets.[26,97,139,140] Decreasing the US pressure threshold has been explored by changing the US parameters in terms of frequency[65,117] or pulse length.[118] Minimizing the mechanical index is often preferred in order to circumvent undesired side effects, but this can compromise the activation of the PCCAs in the acoustic field at depth due to attenuation. A technique called activation pressure matching has been proposed by Rojas et al to deliver the required pressure in order to produce uniform ND vaporization and to limit the delivered amount of energy.[141] They showed that such approach increases the time needed by a single bolus of NDs to generate useful contrast and to provide consistent image enhancement in vivo. Interestingly, Lin et al investigated the contrast enhancement produced by ultrasonically activatable PCCAs, either free or confined in a microvessel or microchannel phantom after US application.[142] Their experimental results indicated more than 1 order of magnitude less acoustic vaporization in a microchannel than that in a free environment taking into account the attenuation effect of the vessel on the MB scattering. This finding may improve the knowledge and the understanding in the applications of PCCAs in vivo.

Beside US, microwave-activated ND vaporization was investigated to overcome the critical issues of traditional ADV. Novel folate-targeted lipid-shelled NDs cored with a mixture of PFCs (ie, PFH, PFP) were prepared for highly efficient percutaneous US imaging-guided microwave ablation of tumors.[143]

Much research has been devoted to the possibility of visualizing the NDs or inducing their vaporization adding other imaging modalities to US. Concurrent optical observation and PAI are the most popular approaches,[81,83,144,145] together with the use of surfactants detectable with MRI.[146,147] Interestingly, phase-change agents have been recently proposed as promising photoacoustic contrast agents. Highly absorbing optical contrast agents, such as gold NPs, can be encapsulated in MBs and NBs for multimodal imaging contrasts. Gold nanospheres have been encapsulated in bovine serum albumin shell of PFC droplet to obtain a dual-contrast agent capable of providing image contrast enhancement for both US and PAI modalities.[148] Other authors reported the preparation of gold NP-templated MBs, filled with various PFC gases, that can generate NDs by a condensation approach.[149]

Very recently, NDs production from homemade, preexisting MBs, based on the use of cosolvents[150] or the acoustic destruction of MBs,[151] has been described by many researchers.

A very appealing idea for future development consists in manufacturing PCCAs directly from already commercially available MBs, such as Definity (Lantheus Medical Imaging)[152] and MicroMarker (Bracco, Geneva, Switzerland and VisualSonics, Toronto, Canada).[63] This strategy is very promising since off-label use of commercially available MBs may be simpler than obtaining FDA or EMA authorizations ex novo.

It is worth noting that the interaction of US pulses with the drug-loaded MBs produced by ADV involves a number of mechanisms, such as acoustic cavitation, heating, radiation forces, and sonoporation.[153] Stable bubble cavitation generates strong shear stress close to the bubble surface, thus impacting on cell membranes. The IC produces shock waves and high-speed microjets, which also disrupt cell membranes. The transient increase in cell membrane permeability allows the uptake of drugs, genes, and peptides from a variety of carriers (polymeric micelles, liposomes, and nanoemulsions).[114]

Intriguingly, the internalization of targeted or nontargeted drug-loaded droplets into cells and the subsequent vaporization

could lead to new tissue-specific therapy, allowing the controlled release of drugs directly to the diseased cells. Studies have shown that lipid-coated MB and liquid PFC droplets can be internalized into neutrophils, macrophages, and tumor cells.[154-157] Preliminary investigations from Kang and colleagues demonstrated the PCCA uptake into peritoneal macrophages.[157]

Conclusions

In summary, future design of theranostic platforms should address many challenges, such as good visualization, high payload, target delivery, and toxicity issues. A number of nanostructures have been developed as effective US imaging tools. Among them, PCCAs might be interesting as multifunctional systems for their specific physicochemical properties and flexible composition. However, further understanding of the NDs behavior as well as the physical mechanisms of ADV either in vitro or in vivo is still needed for the clinical translation.

Acknowledgments

The authors thank Dr Klazina Kooiman and Prof Dr Ir. Nico de Jong from Erasmus Medical Center in Rotterdam for many fruitful discussions and Prof Umberto Lucia from Politecnico of Torino who provided insight and expertise that greatly assisted the research.

Declaration of Conflicting Interests

The author(s) declared no potential conflicts of interest with respect to the research, authorship, and/or publication of this article.

Funding

The author(s) disclosed receipt of the following financial support for the research, authorship, and/or publication of this article: Caterina Guiot and Roberta Cavalli were founded by University of Turin (ex 60%).

ORCID iD

Sara Zullino http://orcid.org/0000-0003-3066-9357

References

1. de Jong N, Emmer M, van Wamel A, Versluis M. Ultrasonic characterization of ultrasound contrast agents. *Med Biol Eng Comput*. 2009;47(8):861–873. doi:10.1007/s11517-009-0497-1.
2. Mariano RN, Alberti D, Cutrin JC, Geninatti Crich S, Aime S. Design of PLGA based nanoparticles for imaging guided applications. *Mol Pharm*. 2014;11(11):4100–4106. doi:10.1021/mp5002747.
3. Huynh E, Lovell JF, Helfield BL, et al. Porphyrin shell microbubbles with intrinsic ultrasound and photoacoustic properties. *J Am Chem Soc*. 2012;134(40):16464–16467. doi:10.1021/ja305988f.
4. Toumia Y, Domenici F, Orlanducci S, et al. Graphene meets microbubbles: a superior contrast agent for photoacoustic imaging. *ACS Appl Mater Interfaces*. 2016;8(25):16465–16475. doi:10.1021/acsami.6b04184.
5. Dove JD, Murray TW, Borden MA. Enhanced photoacoustic response with plasmonic nanoparticle-templated microbubbles. *Soft Matter*. 2013;9(32):7743. doi:10.1039/c3sm51690c.
6. Burns PN, Hope Simpson D, Averkiou MA. Nonlinear imaging. *Ultrasound Med Biol*. 2000;26(suppl 1):S19–S22. doi:10.1016/S0301-5629(00) 00155-1.
7. Buchanan KD, Huang S, Kim H, Macdonald RC, McPherson DD. Echogenic liposome compositions for increased retention of ultrasound reflectivity at physiologic temperature. *J Pharm Sci*. 2008;97(6):2242–2249. doi:10.1002/jps.21173.
8. Liu J, Levine AL, Mattoon JS, et al. Nanoparticles as image enhancing agents for ultrasonography. *Phys Med Biol*. 2006;51(9):2179–2189. doi:10.1088/0031-9155/51/9/004.
9. Luan Y, Faez T, Gelderblom E, et al. Acoustical properties of individual liposome-loaded microbubbles. *Ultrasound Med Biol*. 2012;38(12):2174–2185. doi:10.1016/j.ultrasmedbio.2012.07.023.
10. Kooiman K, Böhmer MR, Emmer M, et al. Oil-filled polymer microcapsules for ultrasound-mediated delivery of lipophilic drugs. *J Control Release*. 2008;133:109–118. doi:10.1016/j.jconrel.2008.09.085.
11. Kothapalli SVVN, Daeichin V, Mastik F, et al. Unique pumping-out fracturing mechanism of a polymer-shelled contrast agent: an acoustic characterization and optical visualization. *IEEE Trans Ultrason Ferroelectr Freq Control*. 2015;62(3):451–462. doi:10.1109/TUFFC.2014.006732.
12. Faez T, Emmer M, Kooiman K, Versluis M, van der Steen A, de Jong N. 20 years of ultrasound contrast agent modeling. *IEEE Trans Ultrason Ferroelectr Freq Control*. 2013;60(1):7–20. doi:10.1109/TUFFC.2013.2533.
13. Huang SL, Hamilton AJ, Nagaraj A, et al. Improving ultrasound reflectivity and stability of echogenic liposomal dispersions for use as targeted ultrasound contrast agents. *J Pharm Sci*. 2001;90(12):1917–1926. doi:10.1002/jps.1142.
14. Alkan-Onyuksel H, Demos SM, Lanza GM, et al. Development of inherently echogenic liposomes as an ultrasonic contrast agent. *J Pharm Sci*. 1996;85(5):486–490. doi:10.1021/js950407f.
15. Huang SL. Liposomes in ultrasonic drug and gene delivery. *Adv Drug Deliv Rev*. 2008;60(10):1167–1176. doi:10.1016/j.addr.2008.03.003.
16. Huang SL, McPherson DD, MacDonald RC. A method to co-encapsulate gas and drugs in liposomes for ultrasound-controlled drug delivery. *Ultrasound Med Biol*. 2008;34(8):1272–1280. doi:10.1016/j.ultrasmedbio.2008.01.005.
17. Huang SL, MacDonald RC. Acoustically active liposomes for drug encapsulation and ultrasound-triggered release. *Biochim Biophys Acta*. 2004;1665(1-2):134–141. doi:10.1016/j.bbamem.2004.07.003.
18. Yin T, Wang P, Zheng R, et al. Nanobubbles for enhanced ultrasound imaging of tumors. *Int J Nanomed*. 2012;7:895–904. doi:10.2147/IJN.S28830.
19. Rapoport N, Gao Z, Kennedy A. Multifunctional nanoparticles for combining ultrasonic tumor imaging and targeted chemotherapy. *J Natl Cancer Inst*. 2007;99(14):1095–1106. doi:10.1093/jnci/djm043.

20. Krupka TM, Solorio L, Wilson RE, Wu H, Azar N, Exner AA. Formulation and characterization of echogenic lipid-pluronic nanobubbles. *Mol Pharm*. 2010;7(1):49–59. doi:10.1021/mp9001816.
21. Hwang TL, Lin YK, Chi CH, Huang TH, Fang JY. Development and evaluation of perfluorocarbon nanobubbles for apomorphine delivery. *J Pharm Sci*. 2009;98(10):3735–3747. doi:10.1002/jps.21687.
22. Peyman SA, McLaughlan JR, Abou-Saleh RH, et al. On-chip preparation of nanoscale contrast agents towards high-resolution ultrasound imaging. *Lab Chip*. 2016;16:679–687. doi:10.1039/c5lc01394a.
23. Reznik N, Williams R, Burns PN. Investigation of vaporized submicron perfluorocarbon droplets as an ultrasound contrast agent. *Ultrasound Med Biol*. 2011;37(8):1271–1279. doi:10.1016/j.ultrasmedbio.2011.05.001.
24. Sheeran PS, Luois S, Dayton PA, Matsunaga TO. Formulation and acoustic studies of a new phase-shift agent for diagnostic and therapeutic ultrasound. *Langmuir*. 2011;27(17):10412–10420. doi:10.1021/la2013705.
25. Cavalli R, Argenziano M, Vigna E, et al. Preparation and in vitro characterization of chitosan nanobubbles as theranostic agents. *Colloids Surf B Biointerfaces*. 2015;129:39–46. doi:10.1016/j.colsurfb.2015.03.023.
26. Sheeran PS, Wong VP, Luois S, et al. Decafluorobutane as a phase-change contrast agent for low-energy extravascular ultrasonic imaging. *Ultrasound Med Biol*. 2011;37(9):1518–1530. doi:10.1016/j.ultrasmedbio.2011.05.021.
27. Chattaraj R, Goldscheitter GM, Yildirim A, Goodwin AP. Phase behavior of mixed lipid monolayers on perfluorocarbon nanoemulsions and its effect on acoustic contrast. *RSC Adv*. 2016;6:111318–111325. doi:10.1039/c6ra20328k.
28. Rapoport NY, Kennedy AM, Shea JE, Scaife CL, Nam KH. Controlled and targeted tumor chemotherapy by ultrasound-activated nanoemulsions/microbubbles. *J Control Release*. 2009;138(3):268–276. doi:10.1016/j.jconrel.2009.05.026.
29. Lee JY, Carugo D, Crake C, et al. Nanoparticle-loaded protein-polymer nanodroplets for improved stability and conversion efficiency in ultrasound imaging and drug delivery. *Adv Mater*. 2015;27(37):5484–5492. doi:10.1002/adma.201502022.
30. Capece S, Domenici F, Brasili F, et al. Complex interfaces in phase-change contrast agents. *Phys Chem Chem Phys*. 2016;18(12):8378–8388. doi:10.1039/C5CP07538F.
31. Martinez HP, Kono Y, Blair SL, et al. Hard shell gas-filled contrast enhancement particles for colour Doppler ultrasound imaging of tumors. *MedChemComm*. 2010;1(4):266–270. doi:10.1039/c0md00139b.
32. Liberman A, Martinez HP, Ta CN, et al. Hollow silica and silica-boron nano/microparticles for contrast-enhanced ultrasound to detect small tumors. *Biomaterials*. 2012;33(20):5124–5129. doi:10.1016/j.biomaterials.2012.03.066.
33. Zhang K, Chen H, Guo X, et al. Double-scattering/reflection in a single nanoparticle for intensified ultrasound imaging. *Sci Rep*. 2015;5(1):8766. doi:10.1038/srep08766.
34. Paris JL, Cabanas MV, Manzano M, Vallet-Reg´ı M. Polymer-grafted mesoporous silica nanoparticles as ultrasound-responsive drug carriers. *ACS Nano*. 2015;9(11):11023–11033. doi:10.1021/acsnano.5b04378.
35. Milgroom A, Intrator M, Madhavan K, et al. Mesoporous silica nanoparticles as a breast-cancer targeting ultrasound contrast agent. *Colloids Surf B Biointerfaces*. 2014;116:652–657. doi:10.1016/j.colsurfb.2013.10.038.
36. Ma M, Chen H, Shi J. Construction of smart inorganic nanoparticle-based ultrasound contrast agents and their biomedical applications. *Sci Bull*. 2015;60(13):1170–1183. doi:10.1007/s11434-015-0829-5.
37. Jin Q, Lin CY, Kang ST, et al. Superhydrophobic silica nanoparticles as ultrasound contrast agents. *Ultrason Sonochem*. 2017;36:262–269. doi:10.1016/j.ultsonch.2016.12.001.
38. Greis C. Ultrasound contrast agents as markers of vascularity and microcirculation, *Clin Hemorheol Microcirc*. 2009;43(1-2):1–9. doi:10.3233/CH-2009-1216.
39. Cosgrove D, Harvey C. Clinical uses of microbubbles in diagnosis and treatment. *Med Biol Eng Comput* 2009;47(8):813–826. doi:10.1007/s11517-009-0434-3.
40. Feinstein SB, Cheirif J, Ten Cate FJ, et al. Safety and efficacy of a new transpulmonary ultrasound contrast agent: initial multicenter clinical results. *J Am Coll Cardiol*. 1990;16(2):316–324. doi:10.1016/0735-1097(90)90580-I.
41. Schneider M. Characteristics of SonoVue. *Echocardiography*. 1999;16(7 pt 2):743–746. doi:10.1111/j.1540-8175.1999.tb00144.x.
42. Kitzman DW, Goldman ME, Gillam LD, Cohen JL, Aurigemma GP, Gottdiener JS. Efficacy and safety of the novel ultrasound contrast agent perflutren (Definity) in patients with suboptimal baseline left ventricular echocardiographic images. *Am J Cardiol*. 2000;86(6):669–674. doi:10.1016/S0002-9149(00)01050-X.
43. Sontum PC. Physicochemical characteristics of sonazoid, a new contrast agent for ultrasound imaging. *Ultrasound Med Biol*. 2008;34(5):824–833. doi:10.1016/j.ultrasmedbio.2007.11.006.
44. Podell S, Burrascano C, Gaal M, Golec B, Maniquis J, Mehlhaff P. Physical and biochemical stability of Optison, an injectable ultrasound contrast agent. *Biotechnol Appl Biochem*. 1999;30(Pt 3):213–223. doi:10.1111/j.1470-8744.1999.tb00773.x.
45. Unger EC, McCreery TP, Sweitzer RH, Caldwell VE, Wu Y. Acoustically active lipospheres containing paclitaxel: a new therapeutic ultrasound contrast agent. *Invest Radiol*. 1998;33(12):886–892. doi:10.1097/00004424-199812000-00007.
46. Tachibana K, Uchida T, Ogawa K, Yamashita N, Tamura K. Induction of cell-membrane porosity by ultrasound. *Lancet*. 1999;353(9162):1409. doi:10.1016/S0140-6736(99)01244-1.
47. van Wamel A, Kooiman K, Harteveld M, et al. Vibrating microbubbles poking individual cells: drug transfer into cells via sonoporation. *J Control Release*. 2006; 112(2):149–155. doi:10.1016/j.jconrel.2006.02.007.
48. Hernot S, Klibanov AL. Microbubbles in ultrasound-triggered drug and gene delivery. *Adv Drug Deliv Rev*. 2008;60(10):1153–1166. doi:10.1016/j.addr.2008.03.005.
49. Cavalli R, Soster M, Argenziano M. Nanobubbles: a promising efficient tool for therapeutic delivery. *Ther Deliv*. 2016;7(2):117–138. doi:10.4155/tde.15.92.

50. Kooiman K, Vos HJ, Versluis M, de Jong N. Acoustic behavior of microbubbles and implications for drug delivery. *Adv Drug Deliv Rev*. 2014;72:28–48. doi:10.1016/j.addr.2014.03.003.
51. Capece S, Chiessi E, Cavalli R, Giustetto P, Grishenkov D, Paradossi G. A general strategy for obtaining biodegradable polymer shelled microbubbles as theranostic devices. *Chem Commun (Camb)*. 2013;49(51):5763. doi:10.1039/c3cc42037j.
52. Fabiilli ML, Haworth KJ, Sebastian IE, Kripfgans OD, Carson PL, Fowlkes JB. Delivery of chlorambucil using an acoustically-triggered perfluoropentane emulsion. *Ultrasound Med Biol*. 2010; 36(8):1364–1375. doi:10.1016/j.ultrasmedbio.2010.04.019.
53. Tang R, Yan F, Yang GY, Chen KM. Microbubbles containing gadolinium as contrast agents for both phase contrast and magnetic resonance imaging. *J Synchrotron Radiat*. 2018;25(pt 2): 5060–5064. doi:10.1107/ S1600577517017404.
54. Ahmed M, Cerroni B, Razuvaev A, et al. Cellular uptake of plain and SPION-modified microbubbles for potential use in molecular Imaging. *Cell Mol Bioeng*. 2017;10(6):537–548. doi:10.1007/ s12195-017-0504-9.
55. Lim AKP, Patel N, Eckersley RJ, et al. Evidence for spleen-specific uptake of a microbubble contrast agent: a quantitative study in healthy volunteers. *Radiology*. 2004;231:785–788. doi:10. 1148/radiol.2313030544.
56. Kabalnov A, Bradley JA, Flaim S, et al. Dissolution of multicomponent microbubbles in the bloodstream: 2. Experiment. *Ultrasound Med Biol*. 1998;24(5):751–760.
57. Yuan F, Dellian M, Fukumura D, et al. Vascular permeability in a human tumor xenograft: molecular size dependence and cutoff size. *Cancer Res*. 1995;55(17):3752–3756. doi:10.1038/ nature02924.
58. Maeda H, Wu J, Sawa T, Matsumura Y, Hori K. Tumor vascular permeability and the EPR effect in macromolecular therapeutics: a review. *J Control Release*. 2000;65(1-2):271–284. doi:10.1016/ S0168-3659(99)00248-5.
59. Couture O, Bevan PD, Cherin E, Cheung K, Burns PN, Foster FS. Investigating perfluorohexane particles with high-frequency ultrasound. *Ultrasound Med Biol*. 2006;32(1):73–82. doi:10. 1016/j.ultrasmedbio.2005.09.010.
60. Lanza GM, Wallace KD, Scott MJ, et al. A novel site-targeted ultrasonic contrast agent with broad biomedical application. *Circulation*. 1996;94(12):3334–3340. doi:10.1161/01.CIR.94.12. 3334.
61. Hughes MS, Marsh JN, Hall CS, et al. Acoustic characterization in whole blood and plasma of site-targeted nanoparticle ultrasound contrast agent for molecular imaging. *J Acoust Soc Am*. 2005;117(2):964–972. doi:10.1121/1.1810251.
62. Apfel RE. Activatable infusable dispersions containing drops of a superheated liquid for methods of therapy and diagnosis. US Patent 5840276. 1998.
63. Sheeran PS, Yoo K, Williams R, Yin M, Foster FS, Burns PN. More than bubbles: creating phase-shift droplets from commercially available ultrasound contrast agents. *Ultrasound Med Biol*. 2017;43(2):531–540. doi:10.1016/j.ultrasmedbio.2016.09.003.
64. Cavalli R, Bisazza A, Trotta M, et al. New chitosan nanobubbles for ultrasound- mediated gene delivery: preparation and in vitro characterization. *Int J Nanomed*. 2012;7:3309–3318. doi:10.2147/ IJN.S30912.
65. Kripfgans OD, Fowlkes JB, Miller DL, Eldevik OP, Carson PL. Acoustic droplet vaporization for therapeutic and diagnostic applications. *Ultrasound Med Biol*. 2000;26(7):1177–1189. doi: 10.1016/S0301-5629(00)00262-3.
66. Martz TD, Sheeran PS, Bardin D, Lee AP, Dayton PA. Precision manufacture of phase-change perfluorocarbon droplets using microfluidics. *Ultrasound Med Biol*. 2012;37(11):1952–1957. doi:10.1016/j.ultrasmedbio.2011.08.012.Precision.
67. Sheeran PS, Luois SH, Mullin LB, Matsunaga TO, Dayton PA. Design of ultrasonically-activatable nanoparticles using low boiling point perfluorocarbons. *Biomaterials*. 2012;33(11): 3262–3269. doi:10.1016/j.biomaterials.2012.01.021.
68. Martin AL, Seo M, Williams R, Belayneh G, Foster FS, Matsuura N. Intracellular growth of nanoscale perfluorocarbon droplets for enhanced ultrasound-induced phase-change conversion. *Ultrasound Med Biol*. 2012;38(10):1799–1810. doi:10.1016/j.ultrasmedbio.2012.05.013.
69. Argenziano M, Banche G, Luganini A, et al. Vancomycin-loaded nanobubbles: a new platform for controlled antibiotic delivery against methicillin-resistant *Staphylococcus aureus* infections. *Int J Pharm*. 2017;523(1):176–188. doi:10.1016/j. ijpharm.2017.03.033.
70. Santos HA, Garc´ıa-Morales V, Roozeman RJ, Manzanares JA, Kontturi K. Interfacial interaction between dextran sulfate and lipid monolayers: an electrochemical study. *Langmuir*. 2005; 21(12):5475–5484. doi:10.1021/la046825u.
71. Giesecke T, Hynynen K. Ultrasound-mediated cavitation thresholds of liquid perfluorocarbon droplets in vitro. *Ultrasound Med Biol*. 2003;29(9):1359–1365. doi:10.1016/S0301-5629(03)00980-3.
72. Mattrey RF. The potential role of perfluorochemicals (PFCS) in diagnostic imaging. *Artif Cells Blood Substit Immobil Biotechnol*. 1994;22(2):295–313. doi:10.3109/10731199409117422.
73. Krafft MP. Fluorocarbons and fluorinated amphiphiles in drug delivery and biomedical research. *Adv Drug Deliv Rev*. 2001; 47(2-3):209–228. doi:10.1016/S0169-409X(01)00107-7.
74. Lattin JR, Pitt WG, Belnap DM, Husseini GA. Ultrasound-induced calcein release from eLiposomes. *Ultrasound Med Biol*. 2012;38(12):2163–2173. doi:10.1016/j.ultrasmedbio.2012.08. 001.
75. Mattrey RF. Perfluorooctylbromide: a new contrast agent for CT, sonography, and MR imaging. *AJR Am J Roentgenol*. 1989; 152(2):247–252. doi:10.2214/ajr.152.2.247.
76. Linstrom PJ, Mallard WG. *NIST Chemistry WebBook*. 2011. doi: 10.5860/CHOICE.35-2709.
77. Freire MG, Carvalho PJ, Queimada AJ, et al. Surface tension of liquid fluorocompounds. *J Chem Eng Data*. 2006;51(5): 1820–1824. doi:10.1021/je060199g.
78. Marin A, Muniruzzaman M, Rapoport N. Acoustic activation of drug delivery from polymeric micelles: effect of pulsed ultrasound. *J Control Release*. 2001;71(3):239–249. doi:10.1016/ S0168-3659(01)00216-4.
79. Sheeran PS, Dayton PA. Improving the performance of phase-change perfluorocarbon droplets for medical ultrasonography:

current progress, challenges, and prospects. *Scientifica (Cairo)*. 2014;2014:579684. doi:10.1155/2014/579684.

80. Sheeran PS, Daghighi Y, Yoo K, et al. Image-guided ultrasound characterization of volatile sub-micron phase-shift droplets in the 20-40 mHz frequency range. *Ultrasound Med Biol*. 2016;42(3): 795–807. doi:10.1016/j.ultrasmedbio.2015.11.012.
81. Paproski RJ, Forbrich A, Huynh E, et al. Porphyrin nanodroplets: sub-micrometer ultrasound and photoacoustic contrast imaging agents. *Small*. 2016;12(3):371–380. doi:10.1002/smll.201502450.
82. Sheeran PS, Matsunaga TO, Dayton PA. Phase-transition thresholds and vaporization phenomena for ultrasound phase-change nanoemulsions assessed via high-speed optical microscopy. *Phys Med Biol*. 2013;58(13):4513–4534. doi:10.1088/0031-9155/58/13/4513.
83. Li S, Lin S, Cheng Y, Matsunaga TO, Eckersley RJ, Tang MX. Quantifying activation of perfluorocarbon-based phase-change contrast agents using simultaneous acoustic and optical observation. *Ultrasound Med Biol*. 2015;41(5):1422–1431. doi:10.1016/j.ultrasmedbio.2014.12.021.
84. Wang CH, Kang ST, Lee YH, Luo YL, Huang YF, Yeh CK. Aptamer-conjugated and drug-loaded acoustic droplets for ultrasound theranosis. *Biomaterials*. 2012;33(6):1939–1947. doi:10.1016/j.biomaterials.2011.11.036.
85. Min HS, You DG, Son S, et al. Echogenic glycol chitosan nanoparticles for ultrasound-triggered cancer theranostics. *Theranostics*. 2015;5(12):1402–1418. doi:10.7150/thno.13099.
86. Dayton PA, Zhao S, Bloch SH, et al. Application of ultrasound to selectively localize nanodroplets for targeted imaging and therapy. *Mol Imaging*. 2006;5(3):160–174. doi:10.2310/7290.2006.00019.
87. Williams R, Wright C, Cherin E, et al. Characterization of submicron phase-change perfluorocarbon droplets for extravascular ultrasound imaging of cancer. *Ultrasound Med Biol*. 2013;39(3): 295–303. doi:10.1016/j.ultrasmedbio.2012.10.004.
88. Reznik N, Lajoinie G, Shpak O, et al. On the acoustic properties of vaporized submicron perfluorocarbon droplets. *Ultrasound Med Biol*. 2014;40(6):1379–1384. doi:10.1016/j.ultrasmedbio.2013.11.025.
89. Reznik N, Shpak O, Gelderblom EC, et al. The efficiency and stability of bubble formation by acoustic vaporization of submicron perfluorocarbon droplets. *Ultrasonics*. 2013;53:1368–1376. doi:10.1016/j.ultras.2013.04.005.
90. Reznik N, Seo M, Williams R, et al. Optical studies of vaporization and stability of fluorescently labelled perfluorocarbon droplets. *Phys Med Biol*. 2012;57(21):7205–7217. doi:10.1088/0031-9155/57/21/7205.
91. Fabiilli MML, Haworth KJK, Fakhri NH, Kripfgans OD, Carson PL, Fowlkes JB. The role of inertial cavitation in acousitc droplet vaporization. *IEEE Trans Ultrason Ferroelectr Freq Control*. 2009;56(5):1006–1017. doi:10.1109/TUFFC.
92. Prato M, Magnetto C, Jose J, et al. 2H,3H-decafluoropentane-based nanodroplets: new perspectives for oxygen delivery to hypoxic cutaneous tissues. *PLoS One*. 2015;10(3):e0119769. doi:10.1371/journal.pone.0119769.
93. Rapoport N, Nam KH, Gupta R, et al. Ultrasound-mediated tumor imaging and nanotherapy using drug loaded, block copolymer stabilized perfluorocarbon nanoemulsions. *J Control Release*. 2011;153(1):4–15. doi:10.1016/j.jconrel.2011.01.022.
94. Yildirim A, Chattaraj R, Blum NT, Goodwin AP. Understanding acoustic cavitation initiation by porous nanoparticles: toward nanoscale agents for ultrasound imaging and therapy. *Chem Mater*. 2016;28(16):5962–5972. doi:10.1021/acs.chemmater.6b02634.
95. Fukumura D, Jain RK. Tumor microvasculature and microenvironment: targets for anti-angiogenesis and normalization. *Microvasc Res*. 2007;74(2-3):72–84. doi:10.1016/j.mvr.2007.05.003.
96. Rapoport N, Kennedy AM, Shea JE, Scaife CL, Nam KH. Ultrasonic nanotherapy of pancreatic cancer: lessons from ultrasound imaging. *Mol Pharm*. 2010;7(1):22–31. doi:10.1021/mp900128x.
97. Kripfgans OD, Orifici CM, Carson PL, Ives KA, Eldevik OP, Fowlkes JB. Acoustic droplet vaporization for temporal and spatial control of tissue occlusion: a kidney study. *IEEE Trans Ultrason Ferroelectr Freq Control*. 2005;52(7):1101–1108. doi:10.1109/TUFFC.2005.1503996.
98. Matsuura N, Williams R, Gorelikov I, et al. Nanoparticle-loaded perfluorocarbon droplets for imaging and therapy. *Proc IEEE Ultrason Symp*. 2009:5–8. doi:10.1109/ULTSYM.2009.5441495.
99. Gao Z, Kennedy AM, Christensen DA, Rapoport NY. Drug-loaded nano/microbubbles for combining ultrasonography and targeted chemotherapy. *Ultrasonics*. 2009;48(4):260–270. doi:10.1016/j.ultras.2007.11.002.
100. Cao Y, Chen Y, Yu T, et al. Drug release from phase-changeable nanodroplets triggered by low-intensity focused ultrasound. *Theranostics*. 2018;8(85):1327–1339. doi:10.7150/thno.21492.
101. Ho YJ, Yeh CK. Concurrent anti-vascular therapy and chemotherapy in solid tumors using drug-loaded acoustic nanodroplet vaporization. *Acta Biomater*. 2017;49:472–485. doi:10.1016/j.actbio.2016.11.018.
102. Marano F, Rinella L, Argenziano M, et al. Targeting taxanes to castration-resistant prostate cancer cells by nanobubbles and extracorporeal shock waves. *PLoS One*. 2016;11(12): e0168553. doi:10.1371/journal.pone.0168553.
103. Magnetto C, Prato M, Khadjavi A, et al. Ultrasound-activated decafluoropentane-cored and chitosan-shelled nanodroplets for oxygen delivery to hypoxic cutaneous tissues. *RSC Adv*. 2014; 4(72):38433–38441. doi:10.1039/C4RA03524K.
104. Ferrara K, Pollard R, Borden M. Ultrasound microbubble contrast agents: fundamentals and application to gene and drug delivery. *Annu Rev Biomed Eng*. 2007;9(1):415–447. doi:10.1146/annurev.bioeng.8.061505.095852.
105. Gao D, Xu M, Cao Z, et al. Ultrasound-triggered phase-transition cationic nanodroplets for enhanced gene delivery. *ACS Appl Mater Interfaces*. 2015;7(24):13524–13537. doi:10.1021/acsami.5b02832.
106. Oddo L, Cerroni B, Domenici F, et al. Next generation ultrasound platforms for theranostics. *J Colloid Interface Sci*. 2017; 491:151–160. doi:10.1016/j.jcis.2016.12.030.
107. Yang H, Zhang C, Li T, et al. Rational design of multifunctional polymeric micelles with stimuli-responsive for imaging-guided combination cancer therapy. *J Biomed Nanotechnol*. 2017; 13(10):1221–1234. doi:10.1166/jbn.2017.2444.

108. Wu Y, Zhou IY, Igarashi T, Longo DL, Aime S, Sun PZ. A generalized ratiometric chemical exchange saturation transfer (CEST) MRI approach for mapping renal pH using iopamidol. *Magn Reson Med*. 2018;79(3):1553–1558. doi:10.1002/mrm.26817.
109. Deng L, Li L, Yang H, et al. Development and optimization of doxorubicin loaded poly(lactic-co-glycolic acid) nanobubbles for drug delivery into Hela cells. *J Nanosci Nanotechnol*. 2014;14(4):2947–2954. doi:10.1166/jnn.2014.8633.
110. Yang H, Deng L, Li T, et al. Multifunctional PLGA nanobubbles as theranostic agents: combining doxorubicin and P-gp siRNA co-delivery into human breast cancer cells and ultrasound cellular imaging. *J Biomed Nanotechnol*. 2015;11(12):2124–2136. doi:10.1166/jbn.2015.2168.
111. Shen X, Li T, Chen Z, et al. Luminescent/magnetic PLGA-based hybrid nanocomposites: a smart nanocarrier system for targeted codelivery and dual-modality imaging in cancer theranostics. *Int J Nanomed*. 2017;12:4299–4322. doi:10.2147/IJN.S136766.
112. Bosca F, Bielecki PA, Exner AA, Barge A. Porphyrin-loaded pluronic nanobubbles: a new us-activated agent for future theranostic applications. *Bioconjug Chem*. 2018;29(2):234–240. doi:10.1021/acs.bioconjchem.7b00732.
113. Zhao H, Wu M, Zhu L, et al. Cell-penetrating peptide-modified targeted drug-loaded phase-transformation lipid nanoparticles combined with low-intensity focused ultrasound for precision theranostics against hepatocellular carcinoma. *Theranostics*. 2018;8(7):1892–1910. doi:10.7150/thno.22386.
114. Zhou Y. Application of acoustic droplet vaporization in ultrasound therapy. *J Ther Ultrasound*. 2015;3(1):20. doi:10.1186/s40349-015-0041-8.
115. Lin CY, Pitt WG. Acoustic droplet vaporization in biology and medicine. *Biomed Res Int*. 2013;2013:404361. doi:10.1155/2013/404361.
116. Kripfgans OD, Fabiilli ML, Carson PL, Fowlkes JB. On the acoustic vaporization of micrometer-sized droplets. *J Acoust Soc Am*. 2004;116(1):272–281. doi:10.1121/1.1755236.
117. Schad KC, Hynynen K. In vitro characterization of perfluorocarbon droplets for focused ultrasound therapy. *Phys Med Biol*. 2010;55(17):4933–4947. doi:10.1088/0031-9155/55/17/004.
118. Lo AH, Kripfgans OD, Carson PL, Rothman ED, Fowlkes JB. Acoustic droplet vaporization threshold: effects of pulse duration and contrast agent. *IEEE Trans Ultrason Ferroelectr Freq Control*. 2007;54(5):933–945. doi:10.1109/TUFFC.2007.339.
119. Kawabata KI, Sugita N, Yoshikawa H, et al. Nanoparticles with multiple perfluorocarbons for controllable ultrasonically induced phase shifting. *Japanese J Appl Phys*. 2005;44(6B):4548–4552. doi:10.1143/JJAP.44.4548.
120. Rapoport NY, Efros AL, Christensen DA, Kennedy AM, Nam KH. Microbubble generation in phase-shift nanoemulsions used as anticancer drug carriers. *Bubble Sci Eng Technol*. 2009;1(1-2):31–39. doi:10.1179/175889709X446516.
121. Shpak O, Verweij M, Vos HJ, de Jong N, Lohse D, Versluis M. Acoustic droplet vaporization is initiated by superharmonic focusing. *Proc Natl Acad Sci U S A*. 2014;111(5):1697–1702. doi:10.1073/pnas.1312171111.
122. Vehkamäki H. *Classical Nucleation Theory Multicomponent Systems*. Berlin/Heidelberg: Springer-Verlag, 2006. ISBN 3540292136. doi:10.1007/3-540-31218-8.
123. Mountford PA, Smith WS, Borden MA. Fluorocarbon nanodrops as acoustic temperature probes. *Langmuir*. 2015;31(39):10656–10663. doi:10.1021/acs.langmuir.5b02308.
124. Mountford PA, Thomas AN, Borden MA. Thermal activation of superheated lipid-coated perfluorocarbon drops. *Langmuir*. 2015;31(16):4627–4634. doi:10.1021/acs.langmuir.5b00399.
125. Wong ZZ, Kripfgans OD, Qamar A, et al. Bubble evolution in acoustic droplet vaporization at physiological temperature via ultra-high speed imaging. *Soft Matter*. 2011;7(8):4009. doi:10.1039/c1sm00007a.
126. Qamar A, Wong ZZ, Fowlkes JB, Bull JL. Dynamics of acoustic droplet vaporization in gas embolotherapy. *Appl Phys Lett*. 2010;96(14):143702. doi:10.1063/1.3376763.
127. Qamar A, Wong ZZ, Fowlkes JB, Bull JL. Evolution of acoustically vaporized microdroplets in gas embolotherapy. *J Biomech Eng*. 2012;0134(3):031010. doi:10.1115/1.4005980.
128. Shpak O, Kokhuis TJA, Luan Y, et al. Ultrafast dynamics of the acoustic vaporization of phase-change microdroplets. *J Acoust Soc Am*. 2013;134(2):1610–1621. doi:10.1121/1.4812882.
129. Plesset MS, Zwick SA. A nonsteady heat diffusion problem with spherical symmetry. *J Appl Phys*. 1952;23(1):95–98. doi:10.1063/1.1701985.
130. Plesset MS, Zwick SA. The growth of vapor bubbles in superheated liquids. *J Appl Phys*. 1954;25(4):493–500. doi:10.1063/1.1721668.
131. Wang T. Rectified heat transfer. *J Acoust Soc Am*. 1974;56(4):1131–1143. doi:10.1121/1. 1903397.
132. Shpak O, Stricker L, Versluis M, Lohse D. The role of gas in ultrasonically driven vapor bubble growth. *Phys Med Biol*. 2013;58(8):2523–2535. doi:10.1088/0031-9155/58/8/2523.
133. Keller JB, Miksis M. Bubble oscillations of large amplitude. *J Acoust Soc Am*. 1980; 68(2):628–633. doi:10.1121/1.384720.
134. Nigmatulin R. *Dynamics of Multiphase Media*. Hemisphere Pub. Corp, 1990. ISBN 089116328X. doi:9780891163282.
135. Hao Y, Prosperetti A. The dynamics of vapor bubbles in acoustic pressure fields. *Phys Fluids*. 1999;11(8):2008–2019. doi:10.1063/1.870064.
136. Pitt WG, Singh RN, Perez KX, et al. Phase transitions of perfluorocarbon nanoemulsion induced with ultrasound: a mathematical model. *Ultrason Sonochem*. 2014;21(2):879–891. doi:10.1016/j.ultsonch.2013.08.005.
137. Rapoport NY, Nam KH, Gao Z, Kennedy A. Application of ultrasound for targeted nanotherapy of malignant tumors. *Acoust Phys*. 2009;55(4-5):594–601. doi:10.1134/S1063771009040162.
138. Fujikawa S, Yano T, Watanabe M. *Vapor–Liquid Interfaces, Bubbles Droplets: Fundamentals Applications*. Berlin, Germany: Springer; 2011. ISBN 9783642180385.
139. Kripfgans OD, Fowlkes JB, Woydt M, Eldevik OP, Carson PL. In vivo droplet vaporization for occlusion therapy and phase aberration correction. *IEEE Trans Ultrason Ferroelectr Freq Control*. 2002;49(6):726–738. doi:10.1109/ TUFFC.2002.1009331.

140. Zhang M, Fabiilli ML, Haworth KJ, et al. Initial investigation of acoustic droplet vaporization for occlusion in canine kidney. *Ultrasound Med Biol*. 2010;36(10):1691–1703. doi:10.1016/j.ultrasmedbio.2010.06.020.
141. Rojas JD, Dayton PA. Optimizing acoustic activation of phase change contrast agents with the activation pressure matching method: a review. *IEEE Trans Ultrason Ferroelectr Freq Control*. 2017;64(1):264–272. doi:10.1109/TUFFC.2016.2616304.
142. Lin S, Zhang G, Leow CH, Tang MX. Effects of microchannel confinement on acoustic vaporisation of ultrasound phase change contrast agents. *Phys Med Biol*. 2017;62(17):6884. doi:10.1088/1361-6560/aa8076.
143. Xu J, Chen Y, Deng L, et al. Microwave-activated nanodroplet vaporization for highly efficient tumor ablation with real-time monitoring performance. *Biomaterials*. 2016;106:264–275. doi:10.1016/j.biomaterials.2016.08.034.
144. Wilson K, Homan K, Emelianov S. Biomedical photoacoustics beyond thermal expansion using triggered nanodroplet vaporization for contrast-enhanced imaging. *Nat Commun*. 2012;3:618. doi:10.1038/ncomms1627.
145. Wilson KE, Wang TY, Willmann JK. Acoustic and photoacoustic molecular imaging of cancer. *J Nucl Med*. 2013;54(11):1851–1854. doi:10.2967/jnumed.112.115568.
146. Astafyeva K, Somaglino L, Desgranges S, et al. Perfluorocarbon nanodroplets stabilized by fluorinated surfactants: characterization and potentiality as theranostic agents. *J Mater Chem B*. 2015;3(14):2892–2907. doi:10.1039/C4TB01578A.
147. Díaz-López R, Tsapis N, Fattal E. Liquid perfluorocarbons as contrast agents for ultrasonography and ^{19}F-MRI. *Pharm Res*. 2010;27(1):1–16. doi:10.1007/s11095-009-0001-5.
148. Wilson SR, Burns PN. Microbubble-enhanced US in body imaging: what role? *Radiology*. 2010;257(1):24–39. doi:10.1148/radiol.10091210.
149. Dove JD, Mountford PA, Murray TW, Borden MA. Engineering optically triggered droplets for photoacoustic imaging and therapy. *Biomed Opt Express*. 2014;5(12):4417. doi:10.1364/BOE.5.004417.
150. Seo M, Williams R, Matsuura N. Size reduction of cosolvent-infused microbubbles to form acoustically responsive monodisperse perfluorocarbon nanodroplets. *Lab Chip*. 2015;15(17):3581–3590. doi:10.1039/C5LC00315F.
151. Blum NT, Yildirim A, Chattaraj R, Goodwin AP. Nanoparticles formed by acoustic destruction of microbubbles and their utilization for imaging and effects on therapy by high intensity focused ultrasound. *Theranostics*. 2017;7(3):694–702. doi:10.7150/thno.17522.
152. Choudhury SA, Xie F, Dayton PA, Porter TR.Acoustic behavior of a reactivated, commercially available ultrasound contrast agent. *J Am Soc Echocardiogr*. 2017;30(2): 189–197. doi:10.1016/j.echo.2016.10.015.
153. Zhou Y. Ultrasound-mediated drug/gene delivery in solid tumor treatment. *J Healthc Eng*. 2013;4(2):223–254. doi:10.1260/2040-2295.4.2.223.
154. Barbarese E, Ho SY, D'Arrigo JS, Simon RH. Internalization of microbubbles by tumor cells in vivo and in vitro. *J Neurooncol*. 1995;26(1):25–34.
155. Dayton PA, Chomas JE, Lum AF, et al. Optical and acoustical dynamics of microbubble contrast agents inside neutrophils. *Biophysical J*. 2001;80(3):1547–1556. doi:10.1016/ S0006-3495(01)76127-9.
156. Yanagisawa K, Moriyasu F, Miyahara T, Yuki M, Iijima H. Phagocytosis of ultrasound contrast agent microbubbles by Kupffer cells. *Ultrasound Med Biol*. 2007;33(2):318–325. doi:10.1016/j.ultrasmedbio.2006.08.008.
157. Kornmann LM, Curfs DM, Hermeling E, et al. Perfluorohexane-loaded macrophages as a novel ultrasound contrast agent: a feasibility study. *Mol Imaging Biol*. 2008;10(5):264–270. doi:10.1007/s11307-008-0146-3.